Macroscopic Principles on the Growth of Wind Waves

著者	Toba Yoshiaki
雑誌名	Science reports of the Tohoku University. Ser. 5, Geophysics
巻	22
号	2
ページ	61-74
発行年	1974-12
URL	http://hdl.handle.net/10097/44719

Sci. Rep. Tôhoku Univ., Ser. 5, Geophysics, Vol. 22, No. 2, pp. 61 to 73, 1974.

*Macroscopic Principles on the Growth of Wind Waves**

YOSHIAKI TOBA

Geophysical Institute, Tôhoku University, Sendai, Japan

(Received October 2, 1974)

Abstract: Wind waves are special phenomena having the characteristics both of water waves and turbulence. A new conception on the growth process of the wind waves is made, not on the standpoint of treating the growth of individual waves deterministically, but on the standpoint of treating the processes macroscopically, and several principles have been obtained. Although very simple, they closely correspond to experimental facts.

Firstly is obtained the three-seconds power law expressed by $H^*=BT^{*3/2}$, where $H^*\equiv gH/u_*^2$ represents the dimensionless significant wave height, normalized by the acceleration of gravity, g, and the friction velocity, u_*, and $T^*\equiv gT/u_*$ the dimensionless significant wave period, and B a universal constant having the value of 6.2×10^{-2}. This is a remarkably fine relation, derived from a hypothetical concept that the dimensionless rate of work done by the wind stress to the wind waves is proportional to the dimensionless wind stress, $u_*^*\equiv u_*^3/g\nu$, where ν represents the kinematic viscosity of air. Using this relation, the significant wave steepness δ is given by $\delta=2\pi BT^{*-1/2}$.

A combination of the three-seconds power law, and the similarity of the spectral form of wind waves, leads to the following concepts on the energy spectrum of wind waves. In the gravity wave range, the gross form of the spectrum is proportional to $gu_*\sigma^{-4}$, where σ is the angular frequency, and the factor of proportionality is 2.0×10^{-2}. The wind waves grow in such a way that the spectrum slides up, keeping its similar form, along the line of the gross form, on the $\log\phi$–$\log\sigma$ diagram, where ϕ is the energy spectrum density. The value of ϕ, at the peak frequency of the fully developed sea, is proportional to $g^2\sigma^{-5}$, the factor of proportionality being 3.8×10^{-3}. The fine structure of the wind waves, in purely controlled conditions such as those in a wind-wave tunnel, shows a characteristic form oscillating around the σ^{-4}-line, and the form is always similar in the gravity wave range. As the wave number becomes large, the effect of surface tension gradually transfers the σ^{-4}-line to a $\sigma^{-8/3}$-line, and the σ^{-5}-line to a $\sigma^{-7/3}$-line.

Concerning the relation of the sea surface wind stress to the state of wind waves, it is shown that the dimensionless roughness parameter, u_*z_0/ν, is determined by a function of two dimensionless parameters: u_*L/ν and $S/\rho_w gL^2$, where L represents the significant wave length, S the surface tension and ρ_w the density of water.

1. Introduction

Examples of stroboscopic pictures, taken in our wind-wave tunnel, of white neutral particles showing path lines of water particles in wind waves, demonstrate that the skin flow is large, and that particles which have been at the surface frequently enter into the subsurface, and particles in the subsurface go up to the surface. When the breaking of wind waves occurs, the turbulent structure of this kind is much more evident. Thus, the standpoint of the present paper is to treat the field of wind waves

---

* Presented at the Symposium on Ocean Waves, Session 1, Wave Dynamics and Prediction, IAMAP/IAPSO Combined First Special Assemblies, Melbourne, Australia, January 22, 1974

in a macroscopic feature, which comes out after reorganized through the turbulence, to obtain macroscopic principles of the growth of wind waves.

The momentum is supplied by the wind to the sea, and enters to waves and current, its working becomes the energy of waves and current, and these physical processes must be determined by the fields of local wind and waves. Namely, the budgets of momentum and energy should be balanced locally. To obtain their quantitative structure in macroscopic forms is the objective of the present paper.

2. Local balance, variables

In a macroscopic expression, the mean wind stress τ, or the mean vertical transport of mean horizontal momentum of the air, per unit horizontal area of the sea surface per unit time, goes partially to waves (τ_w) and partially to current (τ_c), namely,

$$\text{Force:} \quad \underset{\text{(to water)}}{\tau} = \underset{\text{(to wave)}}{\tau_w} + \underset{\text{(to current)}}{\tau_c}. \tag{1}$$

The notation of τ_w is used here for this specific meaning. The working performed by the force to the water is,

$$\text{Working:} \quad \underset{\text{(to water)}}{\tau(u_0+u_c)} = \underset{\text{(to wave)}}{\tau u_0} + \underset{\text{(to current)}}{\tau u_c}. \tag{2}$$

where u_0 is the wave current, or the average horizontal velocity of surface water particles which occurs by the existence of waves, and u_c is the rest of the average water velocity. Consequently, τu_0 goes into the wave energy to become dE/dt:

$$\frac{dE}{dt} = \tau u_0 \cdot Ret\,, \tag{3}$$

where Ret is the retention function and represents the residue of the dissipation of the wave energy.

Now the variables are rearranged. Dimensional variables are the duration t and the fetch F, which are both independent variables; characteristic wave period T, wave height H, τ_w and u_c are dependent variables; τ is considered as the external condition; and there are physical constants g, ρ_w, ρ_a, μ_w, μ_a in the usual meanings, and the surface tension S. There are thirteen variables. But the ratios ρ_w/ρ_a and μ_w/μ_a are constant for given temperature and salinity, so we may eliminate ρ_w and μ_w and use only $\rho(=\rho_a)$ and μ $(=\mu_a)$. We may further eliminate ρ to obtain ν $(=\mu/\rho)$ and u_* $(=\sqrt{\tau/\rho})$ as usual. If we are concerned solely with wind waves, we may construct seven dimensionless variables: the duration $t^*\equiv gt/u_*$ and the fetch $F^*\equiv gF/u_*^2$, which are independent variables, the wave period $T^*\equiv gT/u_*$, the wave height $H^*\equiv gH/u_*^2$ and the ratio $r\equiv\tau_w/\tau$, which are dependent variables, the wind stress $u_*{}^*\equiv u_*{}^3/g\nu$ as the conditioning parameter, and lastly, $S^*\equiv S/\rho_w g^3T^4$ of which the meaning is given later.

3. The three-seconds power law

Now, the working to the waves τu_0 in Eq. (2) is normalized by $\rho g\nu$. Namely, the

u_0 is approximated by the wave current of Stokes wave for the characteristic waves given by

$$u_0 = \kappa^2 a^2 c = \frac{\pi^3 H^2}{g T^3}, \tag{4}$$

where κ is the wave number, a the amplitude and c the phase velocity, then follows

$$\frac{\tau u_0}{\rho g \nu} = \frac{\pi^3 u_*{}^* H^{*2}}{T^{*3}} . \tag{5}$$

Now an assumption is raised: "the dimensionless working to the waves is proportional to $u_*{}^*$ or the dimensionless wind stress" (the second concept of Toba, 1972). It should be noticed that this assumption implies that the working to the waves is related only with wind stress u_*, and not with the present state of waves. Then immediately

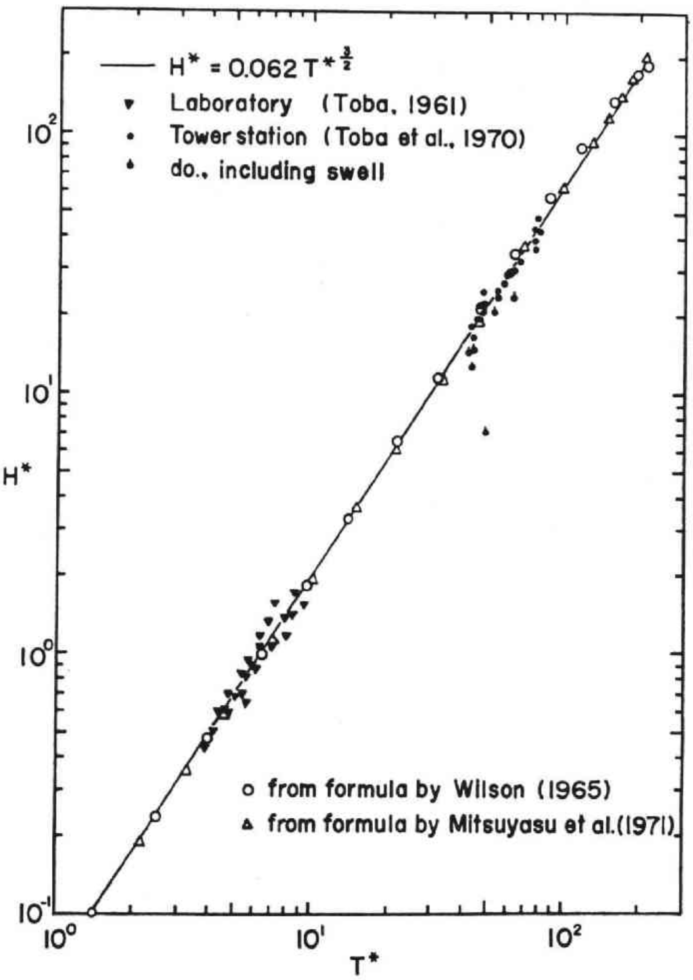

Fig. 1. The three-seconds power law for wind waves.

follows the three-seconds power law:

$$H^* = BT^{*3/2}, \qquad B = 0.062, \tag{6}$$

stating that the H^* is proportional to the three-seconds power of T^*, where B is a universal constant which has been determined by actual data of wind waves.

Figure 1 is an example of the actual data, showing the three-seconds power law. Black triangles are from a wind-wave tunnel experiment (Toba, 1961), black circles are from our observatiou at Shirahama Oceanographic Tower Station (Toba *et al.*, 1971), white circles are points obtained by the use of empirical formulas by Wilson (1965) for significant waves, and white triangles obtained by the use of similar empirical formulas by Mitsuyasu *et al.* (1971). Points for situation including swells show some deviation; otherwise, all of the data here seem to support the three-seconds power law. Figure 1 includes almost full ranges of T^* and H^* for wind waves.

The three-seconds power law is accompanied by the following lemmas.

$$\text{Lemma 1:} \quad u_0 = \pi^3 B^2 u_* = 0.12 u_*, \tag{7}$$

$$\text{Lemma 2:} \quad \frac{H}{L} = \frac{2\pi B}{T^{*1/2}}, \tag{8}$$

and

$$\text{Lemma 3:} \quad \frac{u_* L}{\nu} = \frac{1}{2\pi B} T^{*1/2} \frac{u_* H}{\nu}. \tag{9}$$

The first one postulates that the wave current u_0 is always proportional to u_*. The second one gives the form of steepness. Namely the steepness of significant waves

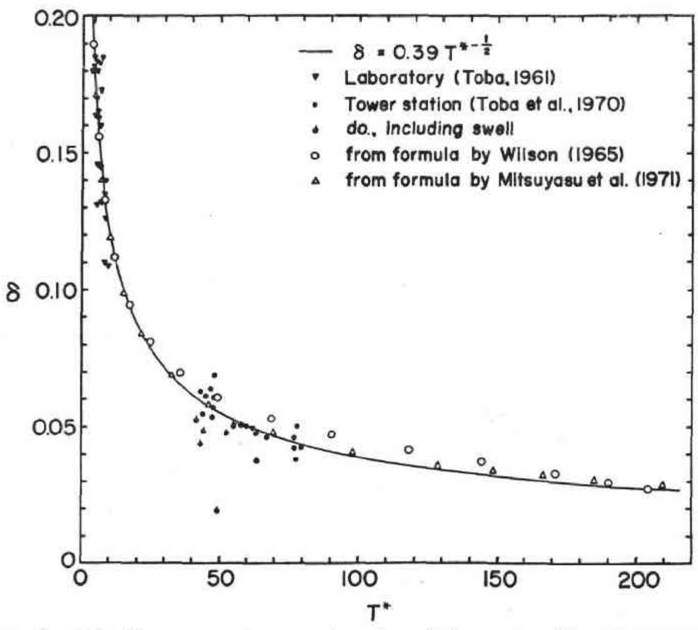

Fig. 2. Lemma 2 of the three-seconds power law for wind waves. The steepness δ is inversely proportional to the root of the dimensionless period T^*.

is inversely proportional to the root of T^*. The third one is the relation between two dimensionless variables: u_*L/ν and u_*H/ν.

In Figure 2 is shown lemma 2. The data is the same with before, and points including swells show again some deviation. The meaning of the three-seconds power law is considered as follows. Firstly, it has diminished the number of dimensionless variables by one, and secondly, it gives an implication about the mechanism of growth of wind waves.

4. Spectral form

Now we proceed to the spectral form of wind waves. The three-seconds power law may be written in a dimensional form by

$$H^2 = B^2 g u_* T^3 . \tag{10}$$

Then we convert T and H to the peak angular frequency σ_p and the spectral density ϕ by

$$\sigma_p = \frac{2\pi}{T} \tag{11}$$

and

$$\int_0^\infty \phi d\sigma = \frac{H^2}{2(2.83)^2} = \frac{H^2}{16} , \tag{12}$$

and see how the point (σ_p, ϕ_p) moves or grows on the logarithmic $(\sigma\text{–}\phi)$-diagram, when the point (T, H) moves on the logarithmic $(T\text{–}H)$-diagram, according to the three-seconds power law.

We assume the similarity of the spectral form of pure wind waves on the logarithmic $(\sigma\text{–}\phi)$-diagram (the fourth concept of Toba, 1973a). Then the normalized ϕ and σ, namely,

$$\phi' = \frac{\phi}{\phi_p} \tag{13}$$

and

$$\sigma' = \frac{\sigma}{\sigma_p} \tag{14}$$

give a constant value of the integration:

$$\int_0^\infty \phi' d\sigma' = \frac{1}{\phi_p \sigma_p} \int_0^\infty \phi d\sigma = \text{constant} = A . \tag{15}$$

From this form, the line, on which the peak point (σ_p, ϕ_p) grows, is obtained as

$$\phi_p = \alpha_p g u_* \sigma_p^{-4} . \tag{16}$$

The value of A, consequently the value of the constant α_p, has been determined by actual data as

$$\alpha_p = \frac{\pi^3 B^2}{2A} = 1.1\pi^3 B^2 = 0.13 . \tag{17}$$

As will be shown later, actual gross forms of the spectra obtained from the wind-wave tunnel lie around a line parallel to the peak's line. Namely, the gross form is given empirically by a similar form given by

$$\phi_g = \alpha_g g u_* \sigma^{-4} \tag{18}$$

and

$$\alpha_g = \frac{1}{6}\pi^3 B^2 = 2.0\times 10^{-2} . \tag{19}$$

The peak point for fully developed sea, or the terminal of the growth of the peak point, is shown here by the subscript 1, or by (σ_1, ϕ_1). Using the empirical value of $T_1{}^*$:

$$T_1{}^* = \frac{2\pi}{\sqrt{C_D}} \times 1.37 , \tag{20}$$

where C_D is the drag coefficient, σ_1 is given by

$$\sigma_1 = \frac{2\pi}{T_1} = \frac{0.029g}{u_*} . \tag{21}$$

Eliminating u_* from Eq. (21) and Eq. (16), since ϕ_1 is the terminal of ϕ_p, the equation of ϕ_1 is given by

$$\phi_1(\sigma_1) = \alpha_1 g^2 \sigma_1{}^{-5} \tag{22}$$

and

$$\alpha_1 = 3.8\times 10^{-3} . \tag{23}$$

The effect of surface tension is expressed by replacing g by

$$g_* \equiv g + \frac{S\kappa^2}{\rho_w} , \tag{24}$$

for infinitesimal waves, where κ is the wave number and may be expressed by σ as the solution of the cubic equation of κ:

$$\frac{S}{\rho_w}\kappa^3 + g\kappa - \sigma^2 = 0 , \tag{25}$$

by the following equation:

$$\kappa = \frac{\sigma_m{}^2}{2g} f(\sigma^*) ,$$

$$f(\sigma^*) = \left\{\sigma^{*2} + \left(\sigma^{*4} + \frac{1}{27}\right)^{1/2}\right\}^{1/3} + \left\{\sigma^{*2} - \left(\sigma^{*4} + \frac{1}{27}\right)^{1/2}\right\}^{1/3} ,$$

$$\sigma^* \equiv \frac{\sigma}{\sigma_m}$$

and

$$\sigma_m = \sqrt{2g}\left(\frac{\rho_w g}{S}\right)^{1/4} . \tag{26}$$

Then the equations for ϕ_p, ϕ_g and ϕ_1 are given by

$$\left.\begin{aligned} \phi_p &= \alpha_p g_* u_* \sigma_p^{-4}, \\ \phi_g &= \alpha_g g_* u_* \sigma^{-4}, \\ \phi_1(\sigma_1) &= \alpha_1 g_*^2 \sigma_1^{-5}, \end{aligned}\right\} \tag{27}$$

and the equations on the $(\phi\text{-}\kappa)$-space are given by

$$\left.\begin{aligned} \phi_{\kappa p} &= \frac{1}{2}\alpha_p g_*^{-1/2} u_* \left(1+\frac{2S\kappa_p^2}{\rho_w g + S\kappa_p^2}\right)\kappa_p^{-5/2}, \\ \phi_{\kappa g} &= \frac{1}{2}\alpha_g g_*^{-1/2} u_* \left(1+\frac{2S\kappa^2}{\rho_w g + S\kappa^2}\right)\kappa^{-5/2}, \\ \phi_{\kappa 1}(\kappa_1) &= \frac{1}{2}\alpha_1 \left(1+\frac{2S\kappa_1^2}{\rho_w g + S\kappa_1^2}\right)\kappa_1^{-3}. \end{aligned}\right\} \tag{28*}$$

For capillary wave range of $g \ll S\kappa^2/\rho_w$, these equations are given by

$$\left.\begin{aligned} \phi_p &= \alpha_p \left(\frac{S}{\rho_w}\right)^{1/3} u_* \sigma_p^{-8/3}, \\ \phi_g &= \alpha_g \left(\frac{S}{\rho_w}\right)^{1/3} u_* \sigma^{-8/3}, \\ \phi_1(\sigma_1) &= \alpha_1 \left(\frac{S}{\rho_w}\right)^{2/3} \sigma_1^{-7/3}, \end{aligned}\right\} \tag{29}$$

and

$$\left.\begin{aligned} \phi_{\kappa p} &= \frac{3}{2}\alpha_p \left(\frac{\rho_w}{S}\right)^{1/2} u_* \kappa_p^{-7/2}, \\ \phi_{\kappa g} &= \frac{3}{2}\alpha_g \left(\frac{\rho_w}{S}\right)^{1/2} u_* \kappa^{-7/2}, \\ \phi_{\kappa 1}(\kappa_1) &= \frac{3}{2}\alpha_1 \kappa_1^{-3}, \end{aligned}\right\} \tag{30**}$$

respectively.

In Figure 3 are shown Eqs. (27). The dotted lines show ϕ_p for three values of u_*. Namely, the peak point grows up on these lines, up to the point where the thick line for ϕ_1 is reached. The gross form is shown by the thin line, for u_* of 50 cm/sec. This is just a vertical displacement of the corresponding dotted line. For σ larger than about 30, the effect of the surface tension is seen.

Figure 4 shows an example of the actual spectra of wind waves, in a wind-wave tunnel. The u_*, determined from the wind profile, is 78.6 cm/sec and the fetch is 6.9 m. The solid line shows the gross form equation, or the ϕ_g-equation, which has a

* Equations (2.26) through (2.28) of Toba (1973a) are revised here according to comments by Mitsuyasu and Honda (1974).

** Equations (2.34) through (2.36) of Toba (1973a) are revised here.

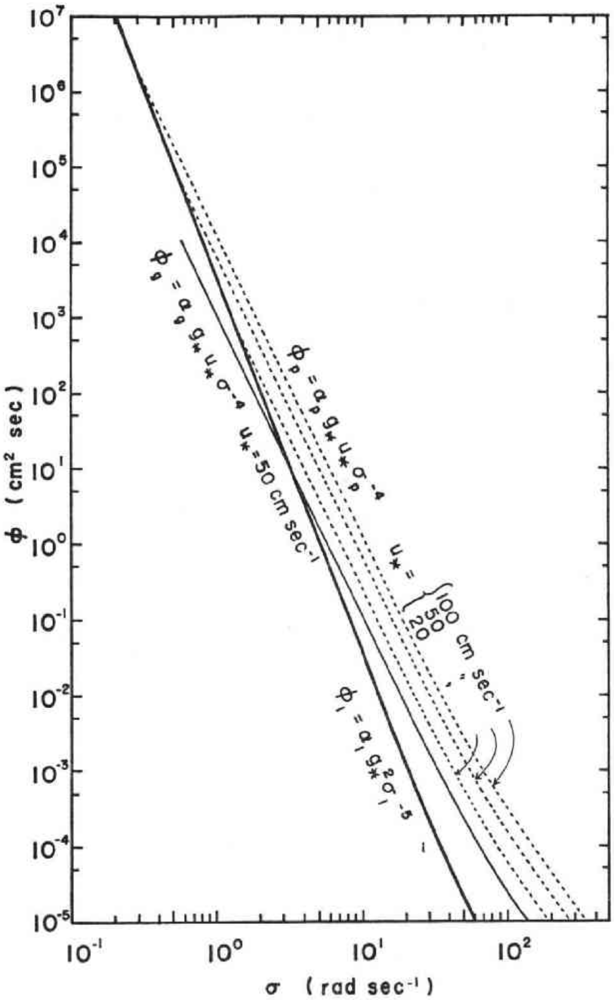

Fig. 3. Peak values of the energy spectra of wind waves grow along the dotted lines, the thick line being the terminal. The thin line is an example of the gross form of the spectrum.

grdient of σ^{-4}, and the broken line indicates the ϕ_1-equation, which has a gradient of σ^{-5}. The gross form of the spectrum lies around the ϕ_g-equation up to large values of σ of 125. Figure 5 shows another example. Quite similar situations may be seen for various combinations of u_* and F.

We may see an oscillating character in the spectrum. Figure 6 shows three different examples of the spectrum, in a normalized presentation. The capillary range is omitted here. The solid line shows again the gross form equation of the gradient of σ^{-4}. The second peak is seen at $2\sigma_p$, and the third at $3\sigma_p$. The entered short lines have gradients of σ^{10} and σ^{-10}, as an empirical fact. When the spectral form grows up along the σ^{-4}-line, the phenomena of overshoot and undershoot may be observed for each fixed frequency, since the spectrum grows in such a way that it slides up, keeping its similar form, along this line of σ^{-4}.

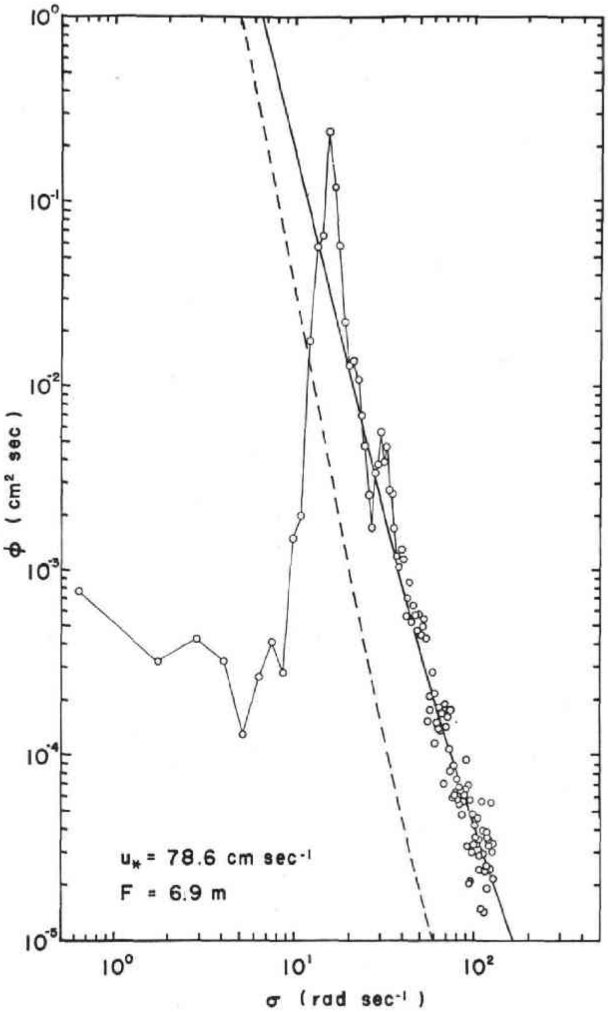

Fig. 4. An example of the energy spectrum of wind waves in a wind-wave tunnel. The solid line shows a σ^{-4}-line for the gross form, and the broken line a σ_1^{-5}-line as a reference.

All of these examples have been taken from wind-wave tunnel experiments, where constant winds blow. In the actual sea, the wind is always fluctuating with space and time. Consequently, the pure spectral form of this kind tends to be obscured.

5. Sea surface wind stress

Now we turn to the problem of the sea surface wind stress. In our treatment so far, u_* has been used as the conditioning parameter. But the problem of drag coefficient C_D, which relates the wind speed to u_*, has been for long time in a confused situation. The problem has three different aspects. The first is the problem of measurement techniques. The second is related to the thermal stratification in the lowest atmosphere. The third is the relation between the wind stress and the present

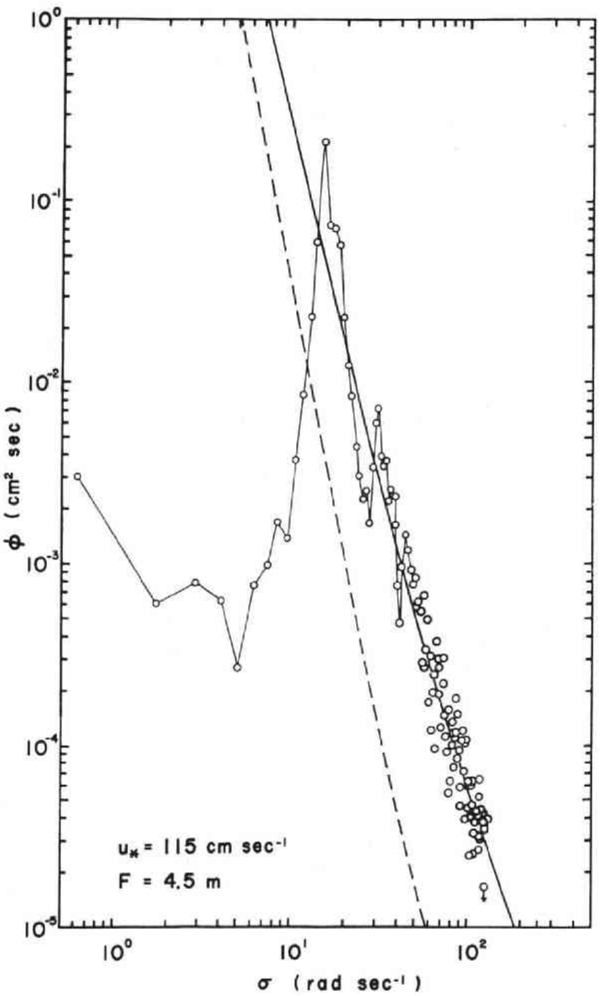

Fig. 5. Another example of the spectrum.

state of wind waves. Here we will confine the problem to the third one.

Over a smooth surface, the dimensionless velocity u/u_* is expressed as a function of the dimensionless height u_*z/ν as is well known:

$$\frac{u}{u_*}=f_1\left(\frac{u_*z}{\nu}\right). \tag{31}$$

Over a rough solid surface, the function should contain two more parameters:

$$\frac{u}{u_*}=f_2\left(\frac{u_*z}{\nu},\ \frac{u_*\epsilon}{\nu},\ \Pi\right), \tag{32}$$

where ϵ is the height of roughness, and Π represents the type of roughness. Over wind waves, these two parameters may be replaced by u_*L/ν and $S/\rho_w g L^2$, namely,

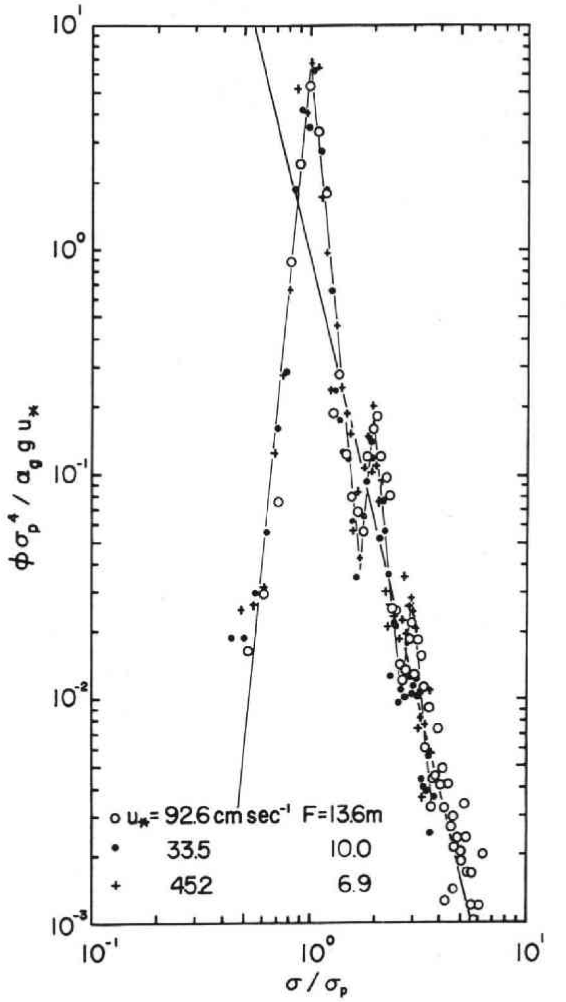

Fig. 6. Three examples of wind wave spectra in the gravity wave range in a normalized form.

$$\frac{u}{u_*} = f_3\left(\frac{u_* z}{\nu}, \frac{u_* L}{\nu}, \frac{S}{\rho_w g L^2}\right), \tag{33}$$

where L is the characteristic or significant wave length.

For Eq. (31), the logarithmic law is obtained as is well known:

$$\frac{u}{u_*} = \frac{1}{k} \ln \frac{u_* z}{\beta \nu}, \qquad \beta = 0.111, \tag{34}$$

where k is von Kármán constant. For Eq. (32), it is modified to

$$\frac{u}{u_*} = \frac{1}{k} \ln \frac{z}{z_0} \tag{35}$$

by introducing z_0, the roughness parameter, which represents the vertical shifting of the logarithmic profile of the flow, and which has a one-to-one correspondence with the drag coefficient C_D by

$$\frac{u_{10}}{u_*}=\frac{1}{\sqrt{C_D}}. \tag{36}$$

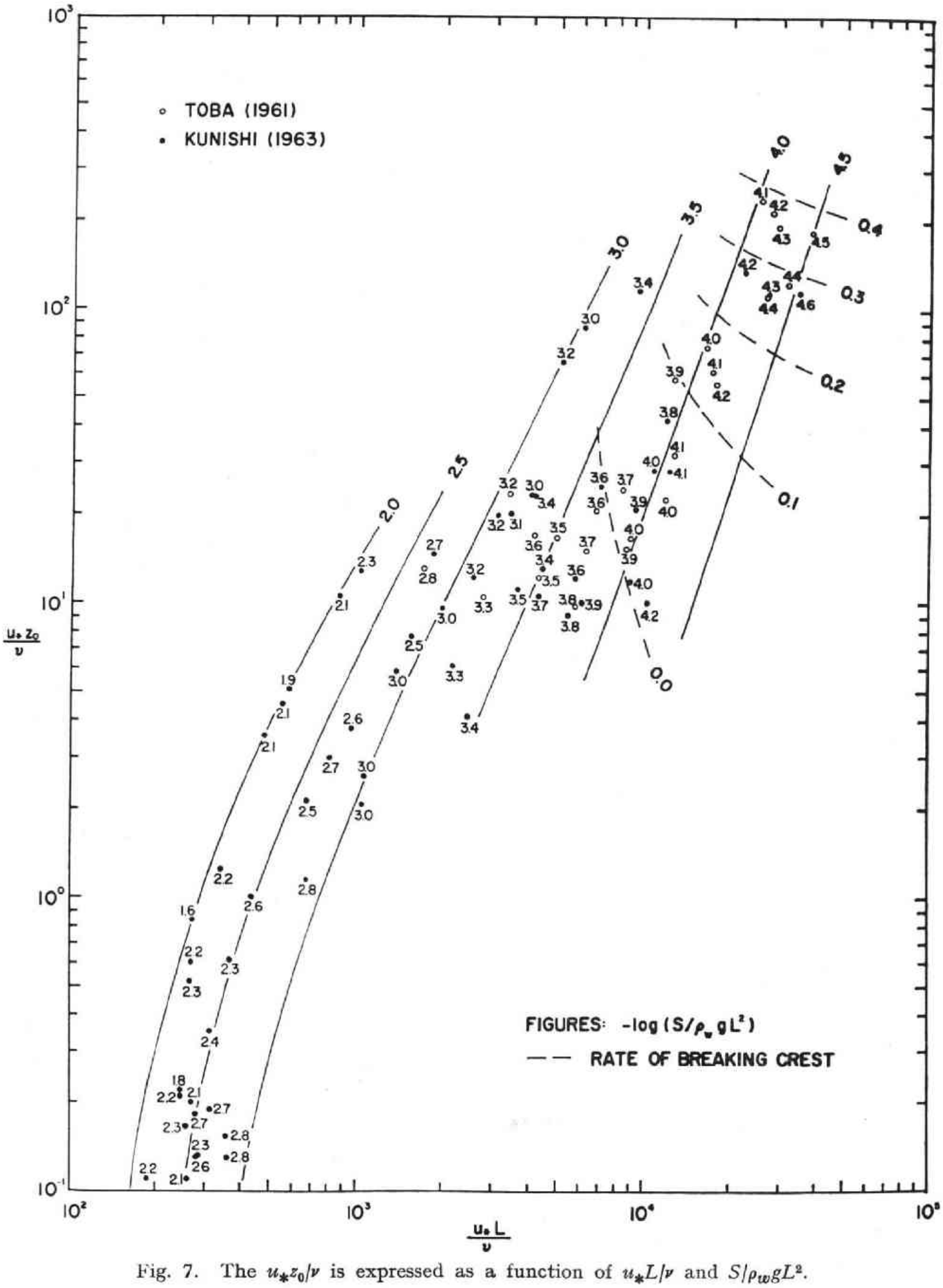

Fig. 7. The u_*z_0/ν is expressed as a function of u_*L/ν and $S/\rho_w gL^2$.

Consequently, the dimensionless roughness parameter $u_* z_0/\nu$ should be a function of $u_* \epsilon/\nu$ and Π:

$$\frac{u_* z_0}{\nu} = fn\left(\frac{u_* \epsilon}{\nu},\ \Pi\right). \tag{37}$$

Over wind waves, this should be a function of u_*^*, T^*, H^*, r, and S^*. However, as already stated, H^* is expressed by T^* by the three-seconds power law. The r is also expressed by T^* (Toba, 1973). Consequently, $u_* z_0/\nu$ should be a function of u_*^*, T^*, and S^*. Corresponding to $u_* \epsilon/\nu$, we may construct $u_* L/\nu$ from u_*^* and T^*. According to lemma 3 of the three-seconds power law, we may also use $u_* H/\nu$ instead of $u_* L/\nu$. Also, S^* corresponds to Π. The S^* or S_L^*:

$$S_L^* \equiv \frac{S}{\rho_w g L^2} \tag{38}$$

has a meaning of the ratio of the surface tension term to the gravity term in Eq. (24), namely,

$$\frac{S\kappa^2}{\rho_w g} = (2\pi)^2 S_L^*. \tag{39}$$

It represents the relative importance of capillary waves in the present state of wind waves. In conclusion, $u_* z_0/\nu$ should be expressed by a function of two dimensionless parameters $u_* L/\nu$ and S_L^*:

$$\frac{u_* z_0}{\nu} = f\left(\frac{u_* L}{\nu},\ \frac{S}{\rho_w g L^2}\right). \tag{40}$$

Figure 7 clearly shows this situation. The data contains wind-wave tunnel experiments by Toba (1961) and by Kunishi (1963). The entered figures show $-\log S_L^*$. At the same time, the broken line indicates the rate of breaking crests. It seems that the rate is also expressed by the two parameters.

References

Kunishi, H., 1963: An experimental study on the generation and growth of wind waves. Disaster Prevention Res. Inst., Kyoto Univ., Bull., No. 61, 41 pp.

Mitsuyasu, H., R. Nakayama and T. Komori, 1971: Observations of the wind and waves in Hakata Bay. Rep. Res. Inst. Appl. Mech., Kyushu Univ., **19**, 37–74.

Mitsuyasu, H. and T. Honda, 1974: The high frequency spectrum of wind-generated waves. J. Oceanog. Soc. Japan, **30**, 185–198.

Toba, Y., 1961: Drop production by bursting of air bubbles on the sea surface (III). Study by use of a wind flume. Memoirs, Coll. Sci., Univ. Kyoto, Ser. A. **29**, 313–344.

Toba, Y., 1972: Local balance in the air-sea boundary processes, I. On the growth process of wind waves. J. Oceanog. Soc. Japan, **28**, 109–120.

Toba, Y., 1973: Local balance in the air-sea boundary processes, II. Partition of wind stress to waves and current. J. Oceanog. Soc. Japan, **29**, 70–75.

Toba, Y., 1973a: Local balance in the air-sea boundary processes, III. On the spectrum of wind waves. J. Oceanog. Soc. Japan, **29**, 209–220.

Toba, Y., H. Kunishi, K. Nishi, S. Kawai, Y. Shimada and N. Shibata, 1971: Study of the air-sea boundary processes at the Shirahama Oceanographic Tower Station. Disaster Prevention Res. Inst., Kyoto Univ., Annals, **14**B, 519–531 (in Japanese).

Wilson, B.W., 1965: Numerical prediction of ocean waves in the North Atlantic for December, 1959. Deutsche Hydro. Zeit., **18**, 114–130.